ORIGINAL RESEARCH

# Hemolysis-induced Lung Vascular Leakage Contributes to the Development of Pulmonary Hypertension

Olga Rafikova[1], Elissa R. Williams[1], Matthew L. McBride[1], Marina Zemskova[1], Anup Srivastava[1], Vineet Nair[2], Ankit A. Desai[2], Paul R. Langlais[1], Evgeny Zemskov[3], Marc Simon[4], Lawrence J. Mandarino[1], and Ruslan Rafikov[1]

[1]Department of Medicine, Division of Endocrinology, and [3]Department of Medicine, Division of Translational and Regenerative Medicine, University of Arizona College of Medicine, Tucson, Arizona; [2]Division of Cardiology, Sarver Heart Center, Department of Medicine, University of Arizona, Tucson, Arizona; and [4]Pittsburgh Heart, Lung, Blood and Vascular Medicine Institute, University of Pittsburgh, Pittsburgh, Pennsylvania

ORCID ID: 0000-0001-5950-4076 (R.R.).

## Abstract

Although hemolytic anemia–associated pulmonary hypertension (PH) and pulmonary arterial hypertension (PAH) are more common than the prevalence of idiopathic PAH alone, the role of hemolysis in the development of PAH is poorly characterized. We hypothesized that hemolysis independently contributes to PAH pathogenesis via endothelial barrier dysfunction with resulting perivascular edema and inflammation. Plasma samples from patients with and without PAH (both confirmed by right heart catheterization) were used to measure free hemoglobin (Hb) and its correlation with PAH severity. A sugen (50 mg/kg)/hypoxia (3 wk)/normoxia (2 wk) rat model was used to elucidate the role of free Hb/heme pathways in PAH. Human lung microvascular endothelial cells were used to study heme-mediated endothelial barrier effects. Our data indicate that patients with PAH have increased levels of free Hb in plasma that correlate with PAH severity. There is also a significant accumulation of free Hb and depletion of haptoglobin in the rat model. In rats, perivascular edema was observed at early time points concomitant with increased infiltration of inflammatory cells. Heme-induced endothelial permeability in human lung microvascular endothelial cells involved activation of the p38/HSP27 pathway. Indeed, the rat model also exhibited increased activation of p38/HSP27 during the initial phase of PH. Surprisingly, despite the increased levels of hemolysis and heme-mediated signaling, there was no heme oxygenase-1 activation. This can be explained by observed destabilization of HIF-1a during the first 2 weeks of PH regardless of hypoxic conditions. Our data suggest that hemolysis may play a significant role in PAH pathobiology.

**Keywords:** pulmonary arterial hypertension; heme; hemoglobin; edema; endothelial barrier

Both pulmonary hypertension (PH) and pulmonary arterial hypertension (PAH) are prevalent in patients with hemolytic anemias, such as sickle cell disease (SCD) (1–3) and thalassemias (4). However, the independent role of hemolysis in PAH development and progression is poorly understood (5).

Hemoglobin (Hb) and its co-factor heme are involved in a wide number of biological processes including gas exchange, antioxidant defense, signal transduction, metabolism, and energy production (6–9). However, the rupture of red blood cells (RBCs) results in the circulation of free Hb, along with its degradation product, heme, which are both toxic for many organs (10). It is now well accepted that extracellular heme and free Hb toxicity plays an important role in several disease conditions associated with hemolysis (e.g., sickle cell disease [11], thalassemia [12], sepsis [13], acute lung injury [14]). Shared pathobiologies in the above-mentioned conditions are related to lung complications, such as hypoxemia and abnormal alveolar–capillary permeability with pulmonary edema. Acute conditions do not induce any reported predisposition to PAH, although, it has been suggested

(Received in original form August 29, 2017; accepted in final form April 13, 2018)

This work was supported by National Institutes of Health (NIH) grants R01HL133085 (O.R.) and Arizona Health Sciences Center Career Development Award (O.R.), and grants R01HL132918 (R.R.) and R01HL136603 (A.A.D.), American Heart Association National Office Scientist Development Grants 14SDG20480354 (R.R.) and 11SDG7670035 (E.Z.), and Arizona Area Health and Education Center grant RG2017-11 (A.S.).

Author Contributions: Conception and design—O.R., A.A.D., E.Z., L.J.M., and R.R.; analysis and interpretation—E.R.W., M.L.M., M.Z., A.S., V.N., P.R.L., and E.Z.; drafting the manuscript for important intellectual content—O.R., P.R.L., M.S., and R.R.

Correspondence and requests for reprints should be addressed to Ruslan Rafikov, Ph.D., Department of Medicine, Division of Endocrinology, University of Arizona College of Medicine, 1501 North Campbell Avenue, Tucson, AZ 85721. E-mail: ruslanrafikov@deptofmed.arizona.edu.

This article has a data supplement, which is accessible from this issue's table of contents at www.atsjournals.org.

Am J Respir Cell Mol Biol Vol 59, Iss 3, pp 334–345, Sep 2018

Originally Published in Press as DOI: 10.1165/rcmb.2017-0308OC on April 13, 2018
Internet address: www.atsjournals.org

that there could be a link with a common molecular and cellular pathways that lead to endothelial cell activation and dysfunction (15). In contrast, chronic hemolytic diseases have a well-documented association with increased pulmonary vascular resistance (PVR) and vascular remodeling seen in patients with PAH (16–19).

Elevated free Hb was previously reported in patients with PAH (20), and there were modest correlations with hemodynamic parameters (mean pulmonary arterial pressure [mPAP], PVR, and cardiac index [CI]). It was found that the highest free Hb had an association with an increased risk of PAH-related hospitalization. However, the molecular mechanisms of free Hb action in PAH were mainly attributed to nitric oxide scavenging activity and induction of oxidative stress. Another study has demonstrated that chronic infusion of Hb into rats can induce a mild form of PH with vascular remodeling (21). This work mainly attributed the Hb effect to the inflammatory responses in the lungs. In the present study, the effect of free Hb and its degradation product, free heme, are explored as the possible contributors to the hemolysis-related effects in PAH development.

Heme moiety is having a renaissance of attention recently as a stand-alone signaling molecule. Free Hb from ruptured RBCs rapidly oxidizes in the bloodstream and releases free heme. Recently, heme was characterized as a molecule that can activate Toll-like receptor (TLR)-4 (22, 23). Activation of TLR4 is involved in the endotoxin-mediated effects on endothelial barrier permeability, and was shown to play an important role in pneumonia, sepsis, and acute lung injury. The TLR4 signaling cascade involves transcriptional activation of many inflammatory genes. However, TLR4-mediated endothelial barrier disruption takes roughly 3–4 hours to reach its maximal effect from endotoxin stimulation (24). In the current study, we have found that the effects of free heme on human lung microvascular endothelial cells (HLMVECs) are at least 10 times faster than those of endotoxin through TLR4 signaling. Thus, we explored other signaling pathways involved in heme-mediated endothelial barrier dysfunction. Here, we report that heme induces endothelial cell permeability through activation of the p38/HSP27 pathway. Increased lung vascular permeability due to hemolysis can contribute to the disease progression in an Sugen (SU)/hypoxia model of PAH and patients with PAH.

## Methods

### Human Subjects

The cohort consisted of patients with a diagnosis of group I PAH with varying functional classes (PAH group, $n = 27$) as well as patients initially suspected of PAH, but not confirmed based on right heart catheterization (non-PAH group, $n = 14$). All patients were prospectively recruited from the University of Arizona and provided written consent to participate in this study with the approval of the University of Arizona Institutional Human Subjects Review Board (Institutional Review Board N1100000621). Clinical and demographic data are presented in Table 1.

### Free Hb Concentration in Plasma

To measure free Hb concentration, we used two methods. The first method involved HPLC separation of the plasma proteins by molecular weight, followed by the quantification of Hb using heme-related absorbance at 400 nm. Briefly, 40 μl of plasma sample was mixed with 60 μl of PBS and injected into a Bio-Rad NGC chromatography system with size exclusion column (ENrichSEC650). A standard, based on porcine Hb (Sigma), was used to identify retention time for the free Hb. The second method involved 1 μl of plasma for seminative gel electrophoresis with the following detection of in-gel heme fluorescence (ex: Blu Epi, em: 532/28 with 100 seconds exposure time). Data were calculated using a Bio-Rad Chemidoc MP imager.

### A Rat Model of PH

All experimental procedures were approved by the University of Arizona Institutional Animal Care and Use Committee. PH was induced by a single injection of SU5416 (50 mg/kg) subcutaneously, followed by 3 weeks of hypoxia (10% $O_2$) and 2 weeks of normoxia. All hemodynamic parameters were obtained similarly to our previous studies (25). This study included four animal groups: control group; SU1, rats were analyzed after 1 week of SU5416 and hypoxia treatment; SU2, rats were analyzed after 2 weeks of SU5416 and hypoxia treatment; and SU5, rats were analyzed after 5 weeks of SU5416 treatment (3 wk of hypoxia with a following 2 wk of normoxia). Sulfasalazine was administered (20 mg/kg intraperitoneal alternate days) starting from Day 7 and continued for 4 weeks. Plasma samples, along with lung and heart tissue, were collected from animals.

### Cell Line

HLMVECs (Sciencell) were cultured using an endothelium media specific for HLMVECs and 10% FBS (Sciencell).

**Table 1.** Demographic and Clinical Characteristics of Patients with and without Pulmonary Arterial Hypertension

| Patient Type | *n* | Sex, Female *N* female (*N* total) | Age (*Yr*) | mPAP (*mm Hg*) | PVR (*Wood Units*) | CI ($L/min/m^2$) | Total Hb (*g/dl*) |
|---|---|---|---|---|---|---|---|
| non-PAH | 14 | 10 (14) | 63 (56–73) | 15 (13–19.5) | 1.7 (1.25–2.2) | 3.01 (2.66–3.43) | 12.7 (10.3–14.9) |
| PAH | 27 | 19 (27) | 58 (49–70) | 41 (31–53)* | 5.35 (3.68–9.18)* | 2.54 (2.27–3.30) | 12.5 (11.7–13.7) |

*Definition of abbreviations*: CI = cardiac index; Hb = hemoglobin; mPAP = mean pulmonary arterial pressure; PAH = pulmonary arterial hypertension; PVR = pulmonary vascular resistance.
The data presented are demographic and clinical data for patients with PAH (World Health Organization group 1) and without PAH involved in this study. Data are presented as median (interquartile range).
*$P < 0.0001$ by Mann-Whitney test.

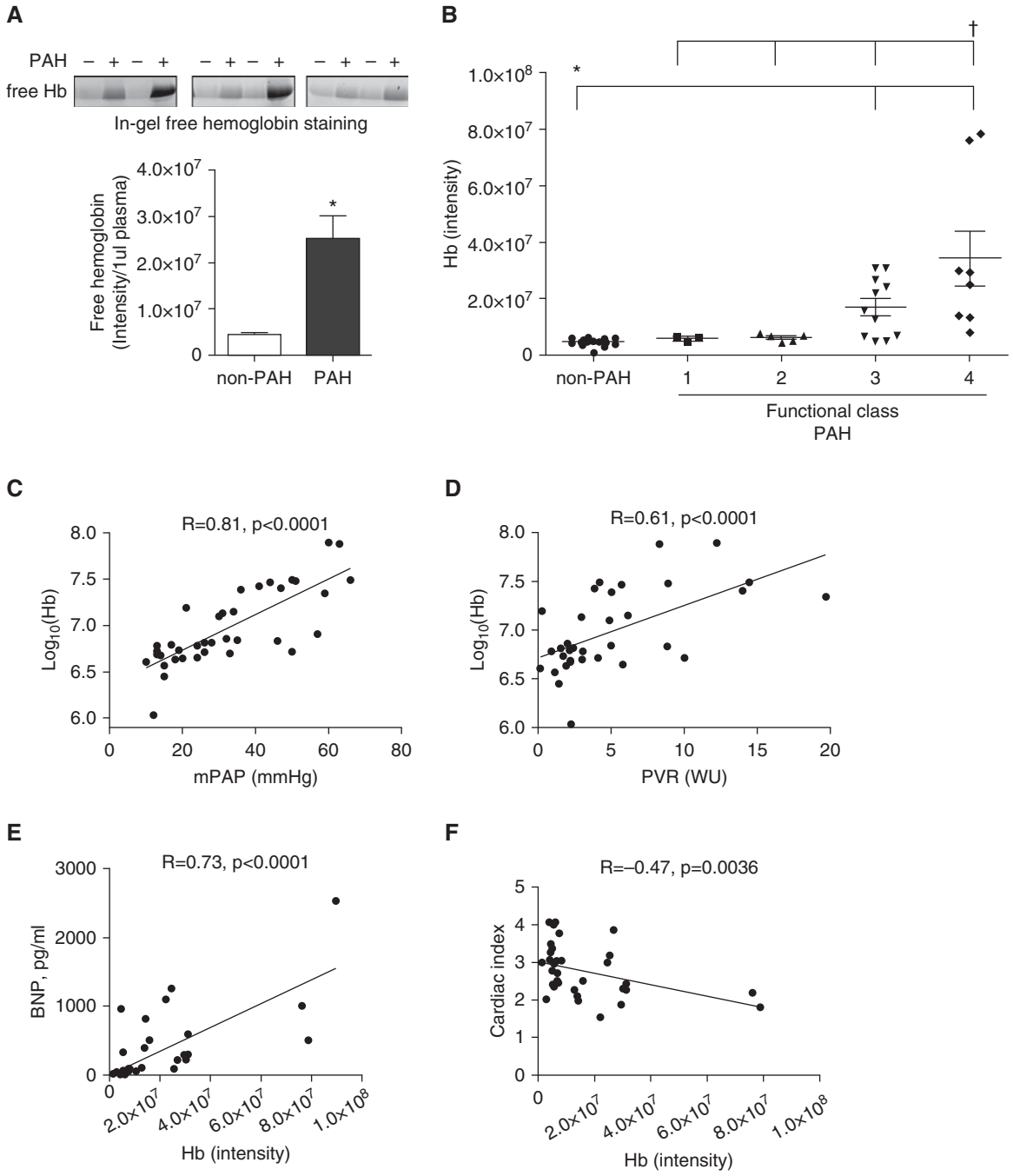


**Figure 1.** Free hemoglobin (Hb) in patients with pulmonary arterial hypertension (PAH). (*A*) Free Hb was monitored by heme fluorescence in the plasma samples (upper panel). Non-PAH control patients ($n = 14$) were preliminarily diagnosed with PAH; however, the diagnosis was not confirmed based on a right heart catheterization. Samples from patients with PAH ($n = 20$) with functional classes (FCs) 3 and 4 were used in the calculation. Our data demonstrate a fivefold increase in free Hb signal in patients with PAH (mean ± SEM, $^*P < 0.0001$ versus non-PAH, Mann-Whitney test). (*B*) The plot of the free Hb by the PAH FC exhibit increased hemolysis with an increase of disease severity. The non-PAH group has a significant difference with PAH FC 3 and 4. Interestingly, PAH FCs 1, 2, and 3 are significantly different from FC 4 (mean ± SEM, $^*P < 0.05$ for non-PAH versus FC3 and -4, $^\dagger P < 0.05$ for FC4 versus FC1, -2, and -3, ANOVA). (*C*) Mean pulmonary arterial pressure (mPAP) strongly correlates with free Hb level (expressed as log(Hb); Spearman's correlation coefficient $r = 0.81$, $P < 0.0001$, $n = 37$). (*D*) Significant correlation between free Hb (expressed as log(Hb)) and pulmonary vascular resistance (PVR) (Spearman's correlation coefficient $r = 0.61$, $P < 0.0001$, $n = 37$). (*E*) Brain natriuretic peptide (BNP) levels as a measure of heart failure correlates with free Hb (Spearman's correlation coefficient $r = 0.73$, $P < 0.0001$, $n = 38$), and (*F*) negative correlation with cardiac index (Spearman's correlation coefficient $r = -0.47$, $P = 0.0036$, $n = 37$) were observed. WU = Wood units.

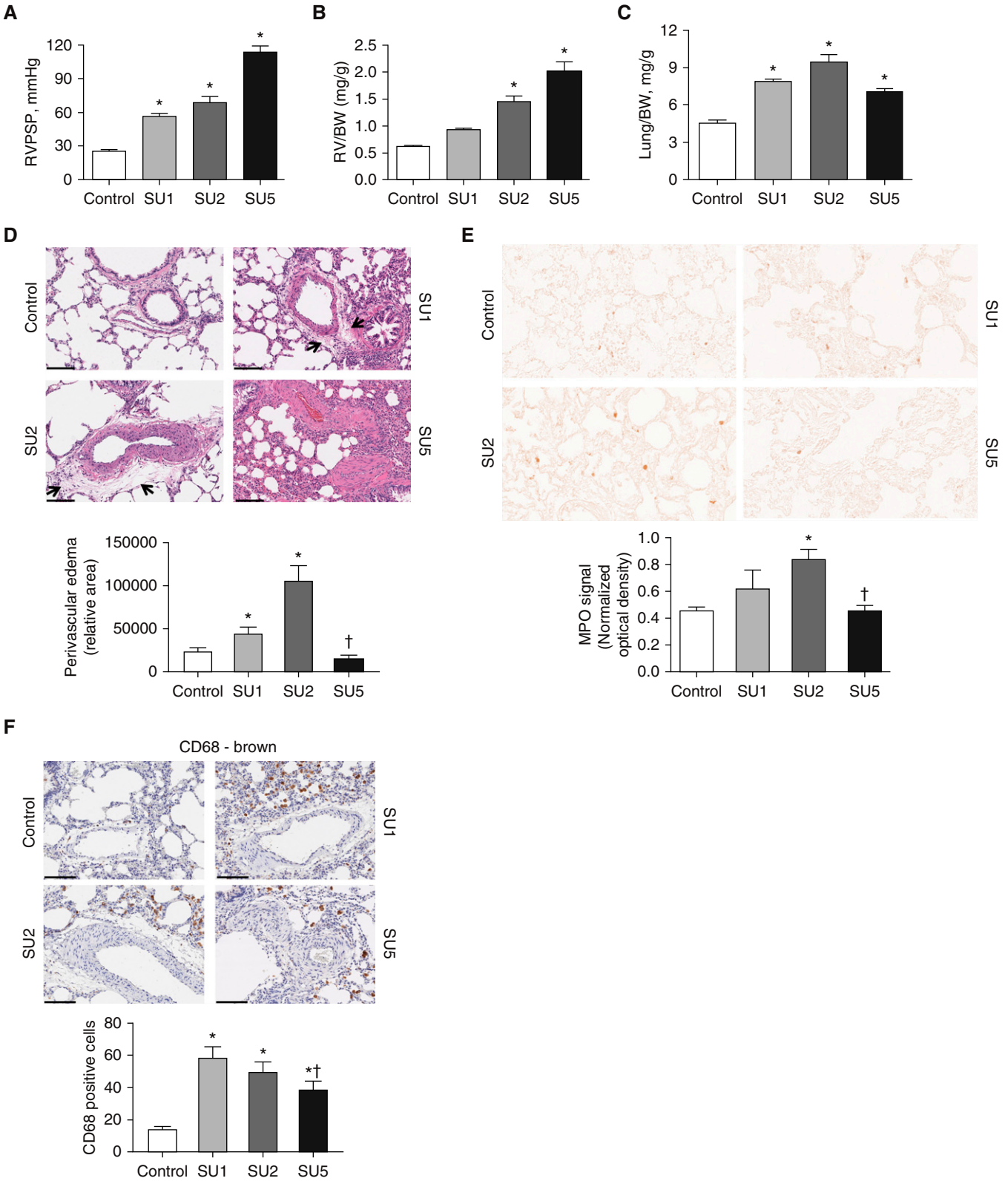


**Figure 2.** Sugen (SU)/hypoxia model of PAH characterized by a lung vascular permeability at an early stage. (*A*) Right ventricular (RV) peak systolic pressure (RVPSP) in rats was measured by the catheterization of the RV. Our data indicate a gradual increase of pressure with disease progression (mean ± SEM, $^*P < 0.05$ versus control group, ANOVA, $n = 6$–8). (*B*) RV hypertrophy was assessed as RV mass over body weight (BW) and expressed in the plot. We found that significant heart hypertrophy started from Week 2 (SU2 group) and continued to increase at Week 5 (SU5) (mean ± SEM, $^*P < 0.05$

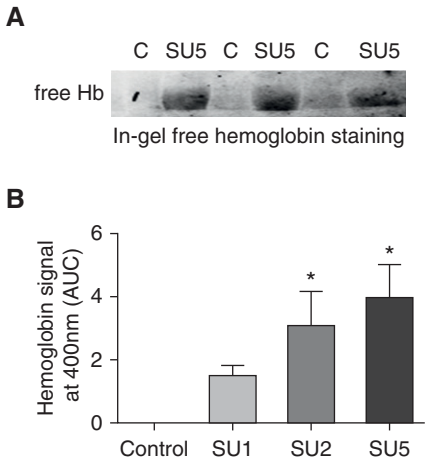


**Figure 3.** Increased free Hb levels in the plasma of SU/hypoxia rats. (*A*) In-gel fluorescent staining of free Hb was obtained for the control and SU5 groups, demonstrating an undetectable level of free Hb in the control group and a marked increase in free Hb in the SU5 group. (*B*) Using HPLC analysis of free Hb content in plasma, we found that free Hb level correlated with disease progression. Control group has no detectable level of free Hb, which was shown to already rise in the SU1 group (not significant) and continued to increase significantly in the SU2 and SU5 groups (mean ± SEM, $^*P < 0.05$ versus control group, ANOVA, $n = 6$–8). AUC = area under curve; C = control.

Cells were used from passages 3–8. All experiments were performed on 100% confluent cells. Any treatments were accompanied with controls treated with a corresponding vehicle.

### Statistical Analysis

An analysis of correlation between plasma free Hb and markers of PAH progression (mPAP, the plasma level of brain natriuretic peptide, PVR, cardiac output, and CI) in cohorts of patients with and without PAH was performed using Spearman's correlation. Unadjusted models assessed the impact of the free Hb on markers of PAH progression. The means (±SEM) were calculated, and significance was determined by the unpaired *t* test, Mann-Whitney test for patient's data, or ANOVA (ANOVA). For ANOVA, Bonferroni's *post hoc* testing was also used. A value of *P* less than 0.05 was considered significant. Statistical calculations were performed using the GraphPad Prism 5 software (GraphPad Software, Inc.).

For all other methodologies, please refer to the materials in the data supplement.

## Results

### Elevated Free Hb Levels in Plasma of Patients with PAH

Fluorescence intensity of free Hb in patients with PAH (PAH functional classes 3 and 4) was plotted against suspected, but not confirmed, patients with PAH (non-PAH group). Interestingly, patients in PAH functional classes (FCs) 3 and 4 demonstrated elevated free Hb compared with those in FC1 and -2. Our data indicate a significant, fivefold elevation of free Hb signals in patients with PAH (Figure 1A). Thus, an increase in Hb plasma content was associated with increased severity of the disease (Figure 1B), as defined by FC. Further analysis of clinical data indicated a strong correlation ($r = 0.81$, $P < 0.0001$) between levels of hemolysis and mPAP in Figure 1C. We also found a significant correlation ($r = 0.61$, $P < 0.0001$) between Hb and PVR (Figure 1D). The levels of circulating brain natriuretic peptide as a measure of right heart failure correlated markedly ($r = 0.73$, $P < 0.0001$) with high Hb levels (Figure 1E). Moreover, free Hb negatively correlated with CI ($r = -0.47$, $P = 0.0036$; Figure 1F). Interestingly, despite the accumulation of free Hb in plasma, the total Hb levels remain unchanged, suggesting the compensation of hemolysis in patients with PAH with increased erythropoiesis, as previously reported (26). These clinical observations lead to the study of the effects of free Hb and heme in an animal model of PAH and cell culture to uncover the mechanistic reasons for the observed correlations.

### Increased Vascular Permeability in the Early Stage of the SU/Hypoxia Model

In the present study, we used a Sugen/hypoxia rat model of PAH. We have used two midpoint groups at Week 1 (SU1) and Week 2 (SU2) after Sugen administration and the final time point at Week 5 (SU5). Right ventricle (RV) catheterization indicates a significant increase in the RV peak systolic pressure (RVPSP) as early as Week 1 (SU1) and development of a severe form of PAH (RVPSP at 115 mm Hg) in the SU5 group (Figure 2A). RV hypertrophy (measured as RV mass normalized to the body weight, as left ventricle was found to be also hypertrophied at the late stages) showed a significant increase in the SU2 group with a further progression of RV hypertrophy in the SU5 group (Figure 2B). Interestingly, the lung weight increased only at the very early stages of PAH in SU1 and SU2 (Figure 2C). Aberrant changes in the lung weight suggested the development of lung edema during the early stages of the disease, and it was previously reported in the monocrotaline model of PAH (27, 28).

The histological comparison revealed a significantly pronounced perivascular space edema, specifically in SU1 and SU2 animals (Figure 2D). Importantly, in the late stage of the PAH, the highly proliferative vessels, but not perivascular edema, were observed. Indeed, the proliferation of the vascular wall can decrease the vascular leakage due to increased numbers of cell layers that fluids should cross. This may explain the drop in the lung weight in the SU2 versus the SU5 group (Figure 2C).

**Figure 2.** (Continued). versus control group, ANOVA, $n = 6$–8). (*C*) Interestingly, lung weight per BW values do not follow a similar steady increase with disease progression. Instead, they increase significantly early in the SU1 and SU2 groups and decrease at SU5, even below SU1 values. Aberrant changes in lung weight can be attributed to lung edema development at SU1 and SU2, with a resolution at SU5 (mean ± SEM, $^*P < 0.05$ versus control group, ANOVA, $n = 6$–8). (*D*) Indeed, histological analyses of lungs revealed increased perivascular edema in SU1 and SU2 groups (arrows). Blinded quantification of edema for arteries with sizes of 50–200 μm showed a significant increase in edema area for the SU1 and -2 groups (mean ± SEM, $^*P < 0.05$ versus control group, $^\dagger P < 0.05$ for SU2 versus SU5, ANOVA, $n = 6$–8). (*E*) Double-blinded analysis of random lung fields stained for myeloperoxidase (MPO) exhibited increased neutrophils infiltration in the early stage of disease, with a significant difference in the SU2 group and resolution in the SU5 group (mean ± SEM, $^*P < 0.05$ versus control group, $^\dagger P < 0.05$ for SU2 versus SU5, ANOVA, $n = 6$–8). (*F*) Perivascular accumulation of activated (CD68-positive) macrophages markedly increased in the SU1 and SU2 groups. However, SU5 also had increased perivascular macrophage staining (mean ± SEM, $^*P < 0.05$ versus control group, $^\dagger P < 0.05$ for SU1 versus SU5, ANOVA, $n = 6$–8). Scale bars: 100 μm (*D* and *F*). *E* magnification is ×40.

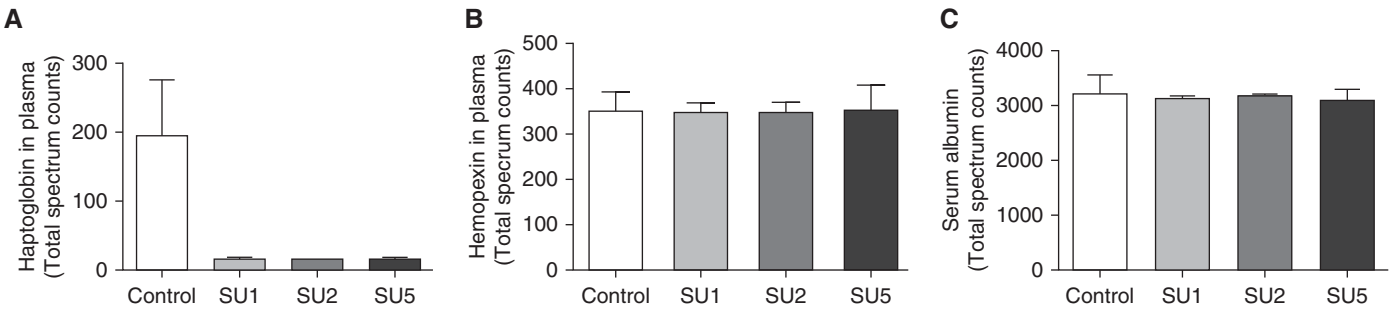


**Figure 4.** Haptoglobin depletion in the Su/hypoxia model. Rat plasma samples separated by gel electrophoresis were assayed by mass spectrometry to profile the plasma proteome for protein abundance changes across different stages of the disease. (*A*) Our data indicate that relative abundance of haptoglobin (expressed as total spectra counts) markedly decreased in disease (~10-fold decrease). (*B*) Hemopexin plasma content was unchanged between groups. (*C*) Serum albumin total spectra counts were used to ensure equal loading and processing of the samples.

Lung sections also possessed a significant accumulation of myeloperoxidase-stained neutrophils in the SU1 and SU2 groups, but not the SU5 group (Figure 2E). This increase in infiltration of inflammatory cells correlated with our observation of the lung leakage shown in Figures 2C and 2D. Immunostaining of the lungs against CD68, a marker of activated macrophages, indicated perivascular localization of activated macrophages in all groups (Figure 2F). Overall, the data indicate the increased permeability of the pulmonary vascular wall, especially at an early stage of PAH.

### Free Hb in an SU/Hypoxia Model

To quantify the concentration of free Hb in the SU/hypoxia model, we used two different methods. First, we used in-gel Hb staining that showed no free Hb staining in controls and a high level of accumulation in the SU5 group (Figure 3A). Using the HPLC method of Hb detection, we found that there was a significant and gradual increase in free Hb in all SU-treated groups that correlated with an increase of pulmonary pressure and a disease progression (Figures 2A and 3B). Analysis of plasma proteome revealed a reduction of plasma haptoglobin content that highlights hemolysis (29) in the SU/hypoxia model (Figure 4A). We have also found that hemopexin levels during disease progression were unchanged (*see* Figure 4B). Hemopexin can be induced when the heme concentration is high (30). Thus, the rate of hemopexin recycling can be matched with hemopexin upregulation resulting in the same plasma levels. Importantly, serum albumin levels were identical in all samples that indicate equal loading and processing of the samples in the proteomic analysis (Figure 4C).

### Heme-mediated Endothelial Barrier Permeability

Hb undergoes rapid oxidation in the bloodstream (31). Oxidized Hb releases its cofactor, heme, which could affect the endothelial barrier, and explains our observation of the lung leakage in the animal model. In this experiment, we studied the effect of free heme on HLMVEC barrier function using ECIS measurements of transendothelial electrical resistance (TEER). A gradual increase in free heme (0, 5, 10, 20, and 50 μM) added to the HLMVEC decreases endothelial monolayer barrier function, with a maximum antibarrier activity after 10–20 minutes of heme addition to the cells (Figure 5A). Interestingly, the heme-mediated barrier disruption had a recovery time of approximately 1 hour after heme administration for the 5- and 10-μM concentrations; however, 50 μM heme did not recover back to the control level.

### Effect of Heme on p38 and HSP27 Phosphorylation

Our data in Figure 5A indicate that heme has a rapid effect on the endothelial barrier. In this experiment, we tested whether activation of stress response components, p38 mitogen-activated protein kinase (MAPK) and p38-mediated phosphorylation of barrier-disruptive HSP27 could be responsible for heme-mediated effects on HLMVEC barrier function. We found that free heme incubation (30 min) with HLMVEC can induce p38 activation with as little as 1 μM of heme (Figure 5B). Our data exhibited the dose dependence of p38 activation by different heme concentrations.

To test whether activation of p38 MAPK is consistent with phosphorylation levels of HSP27, we monitored both proteins at different time points. Our data indicate that level of p38 activation by heme (50 μM) is correlated with phosphorylation of HSP27 (Figure 5C). Moreover, this activation of HSP27 is increased even after 45 minutes from heme addition (Figure 5C). To test whether heme-induced p38 activation is involved in barrier disruption, we used electric cell-substrate impedance sensing (ECIS) measurements of TEER in an HLMVEC culture model to assess barrier function under these conditions. Inhibition of p38 signaling with SB 239,063 (10 μM) resulted in attenuation of heme-mediated endothelial barrier disruption (Figure 5D)

### Activation of a Heme-mediated Pathway via Heme Carrier Protein-1–Assisted Translocation

Heme's involvement in the rapid intracellular signaling suggests that heme is actively transported through the plasma membrane. Heme carrier protein (HCP)-1 was reported to assist heme translocation in intestinal epithelial cells (32), and was also found in the endothelial cell membrane. By using sulfasalazine (125 and 250 μM), a small molecule inhibitor of HCP-1, we tested the involvement of HCP-1 in heme-mediated effects on the endothelial barrier using ECIS. It was found that pretreatment (30 min) with sulfasalazine significantly and dose dependently decreased the effect

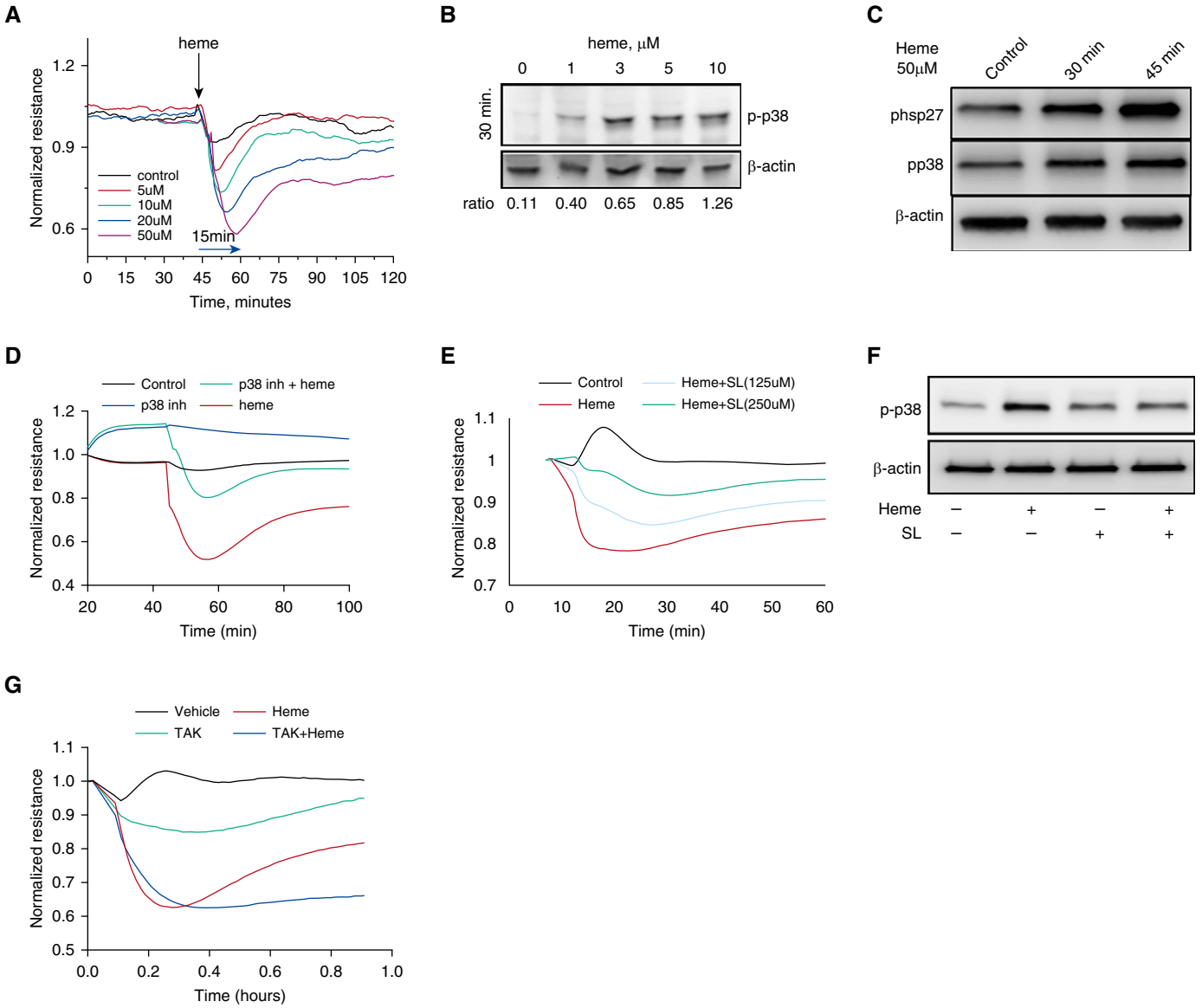


**Figure 5.** Heme-mediated permeability in human lung microvascular endothelial cells (HLMVECs) involves activation of the p38/HSP27 pathway. (*A*) HLMVECs were treated with heme at four different concentrations (5, 10, 20, and 50 μM) in the ECIS instrument that measures transendothelial electrical resistance. A drop in the resistance reflects increased endothelial layer permeability. Our data indicate an immediate, dose-dependent, and rapid (reaching nadir within 15 min) drop in the endothelial barrier function of HLMVECs treated with heme (averaged values from three experiments). (*B*) In the search for the possible stress response elements involved, we examined phosphorylation at Threonine 180 and Tyrosine 182 p38 mitogen-activated protein kinase (MAPK) and found a robust increase in p38 activation in HLMVECs in response to heme. (*C*) p38 MAPK is an upstream kinase for HSP27, which results in phosphorylation of HSP27 at serine 82 (S82), leading to endothelial barrier disruption events. Our Western blot data indicate a unidirectional time-dependant increase in p38 and HSP27 activities by heme (50 μM) treatment (experiments were performed in triplicate). (*D*) Inhibitor of p38 MAPK, SB 239,063 (10 μM), was given 30 minutes before heme (50 μM) and resulted in significant attenuation of heme-mediated barrier dysfunction in HLMVECs. (*E*) To study a possible role of heme transporter—heme carrier protein (HCP)-1—we used a pharmacological inhibitor of HCP-1, sulfasalazine (SL) (125 and 250 μM), to pretreat HLMVECs before heme addition (30 min). Our endothelial barrier data showed sulfasalazine protection from heme-mediated endothelial barrier dysfunction (averaged values from three experiments). (*F*) Pretreatment of HLMVECs with sulfasalazine (20 μM, 30 min) decreased heme-mediated (50 μM) activation of p38 MAPK, as indicated by Western blot data (experiments were performed in triplicate). (*G*) Toll-like receptor-4 inhibitor, TAK-242 (100 nM), pretreatment of HLMVECs 30 minutes before heme addition did not show an effect on heme-mediated permeability (averaged values from three experiments).

of the heme (Figure 5E). Sulfasalazine pretreatment also prevented heme-mediated activation of p38 MAPK, as indicated by Western blot (Figure 5F). To demonstrate the contribution of extracellular heme signaling via activation of TLR4 (22), we pretreated HLMVECs with TAK-242 (100 nM), a TLR4 antagonist, and performed ECIS measurements of TEER. TAK-242 did not alter the heme-mediated drop in endothelial barrier (Figure 5G).

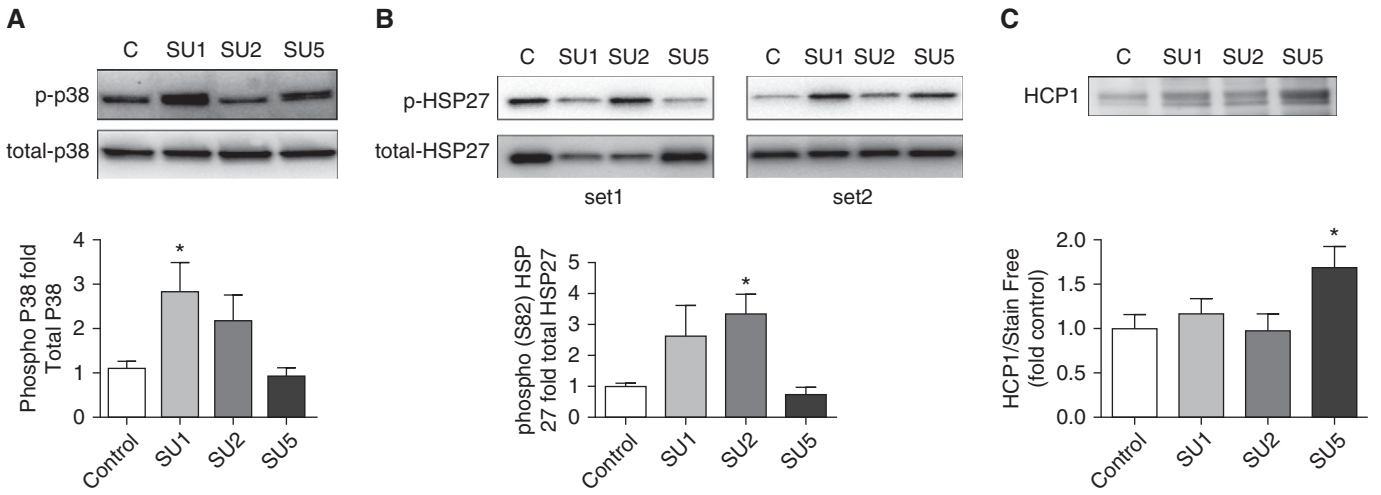


**Figure 6.** Activation of the p38/HSP27 pathway in the SU/hypoxia model at an early stage of the disease. (*A*) Western blot analysis of the lung tissues exhibited fast (in the SU1 group) activation of p38 MAPK signaling in the SU/hypoxia model. Normalization of this signaling back to control levels at Week 5 (SU5) was observed (mean ± SEM, $^*P < 0.05$ versus control group, ANOVA, $n = 6$). (*B*) Our data indicate increased p38-dependent phosphorylation of HSP27 at serine 82 in Weeks 1 and 2 (SU1 [not significant] and SU2 [significant]) in lung tissues. Phosphorylation of HSP27 in the SU5 group was similar to that in the control group. Owing to the variability in phospho-HSP27 signaling, we used two independent sets for illustration (mean ± SEM, $^*P < 0.05$ versus control group, ANOVA, $n = 6$). (*C*) Interestingly, HCP-1 expression was upregulated only at the end stage of disease in the SU5 group. Gel loadings were normalized with the stain-free methods of total protein measurement; *see* Figure E1 in the data supplement (mean ± SEM, $^*P < 0.05$ versus control group, ANOVA, $n = 6$).

### p38/HSP27 Signaling in an SU/hypoxia Model

Studies were performed to confirm that p38/HSP27 signaling pathway takes place in an SU/hypoxia animal model, where we see lung leakage and increased hemolysis. Our Western blot data indicated significant levels of phospho-p38 in the SU1 group and elevated, but not statistically significant, changes in the SU2 group (Figure 6A). In contrast, the late stage of PAH demonstrated a near-control level of p38 MAPK activation, which is highly correlated with changes in the lung permeability (Figures 2C and 2E).

Moreover, in accordance with our cell culture data (Figure 5C), phopsho-HSP27 levels were increased in the SU1 group and significantly upregulated in the SU2 group (Figure 6B). Importantly, activation of HSP27 was back to normal at SU5.

To check whether increased activation of heme-mediated pathways can be explained by the upregulated expression of HCP-1, we analyzed lung tissue with staining against HCP-1. Although HCP-1 was expressed in the lungs in all our animal groups, there was an additional upregulation in the SU5 group (Figure 6C).

### Heme Scavenging by Heme Oxygenase-1 in an SU/Hypoxia Model

To further delineate why heme-activated signaling through the p38/HSP27 pathway works only at the early stage of PH, we tested heme oxygenase (HO)-1 activity. HO-1 is an intracellular heme-scavenging system that usually is inducible by high heme levels and consumes heme with a production of biliverdin/bilirubin. First, we have found that HO-1 levels did not change at Week 1, was significantly reduced at Week 2, and was then markedly elevated at Week 5 (Figure 7A). This finding corresponds with our previous observations that heme-mediated signaling is occurring specifically in SU1 and SU2 groups and is diminished in the SU5 group. To confirm our Western blot data, we have also monitored the bilirubin levels in lungs to assess the HO-1 activity. It was found that bilirubin levels correspond to our HO-1 expression data, with the highest concentration in the SU5 (Figure 7B).

It is well accepted that HO-1 expression is regulated by HIF-1a (33). Thus, we evaluated the HIF-1a protein level in lungs. Importantly, our Western blot data indicate the same trend for HIF-1a expression (Figure 7C) as we found for HO-1 (Figure 7A), suggesting that nonresponsiveness of HO-1 to the elevated hemolysis may be explained by the decreased stability of HIF-1a in the SU1 and SU2 groups. Low HIF-1a concentration could be explained by its degradation during surgical procedures on rats; thus, to additionally confirm the level of HIF-1a activity, we have measured erythropoietin (EPO) plasma levels, a well-established downstream product of HIF-1a activity (34). Indeed, we found that EPO did not change during hypoxia, and was highly elevated only during normoxia (SU5) (Figure 7D). Therefore, all four experiments in Figures 7A–7D showed a reduced level of HIF-1a activity in the SU1 and SU2 groups in spite of hypoxic conditions during the first 3 weeks of the SU/hypoxia model. To better understand why HIF-1a is downregulated under hypoxia, we assayed the level of expression for VHL and ELNG2 (PDH) proteins, which are responsible for HIF-1a degradation. Our data indicate upregulation for both proteins (Figures 7E and 7F). Importantly, carbonic anhydrase IX, which overexpress in the hypoxic tissue to recycle increased $CO_2$, indicated increased levels in the first 2 weeks (SU1 and SU2), with a decrease to a normal level at Week 5 (Figure 7G), in accordance to the hypoxia/normoxia schedule.

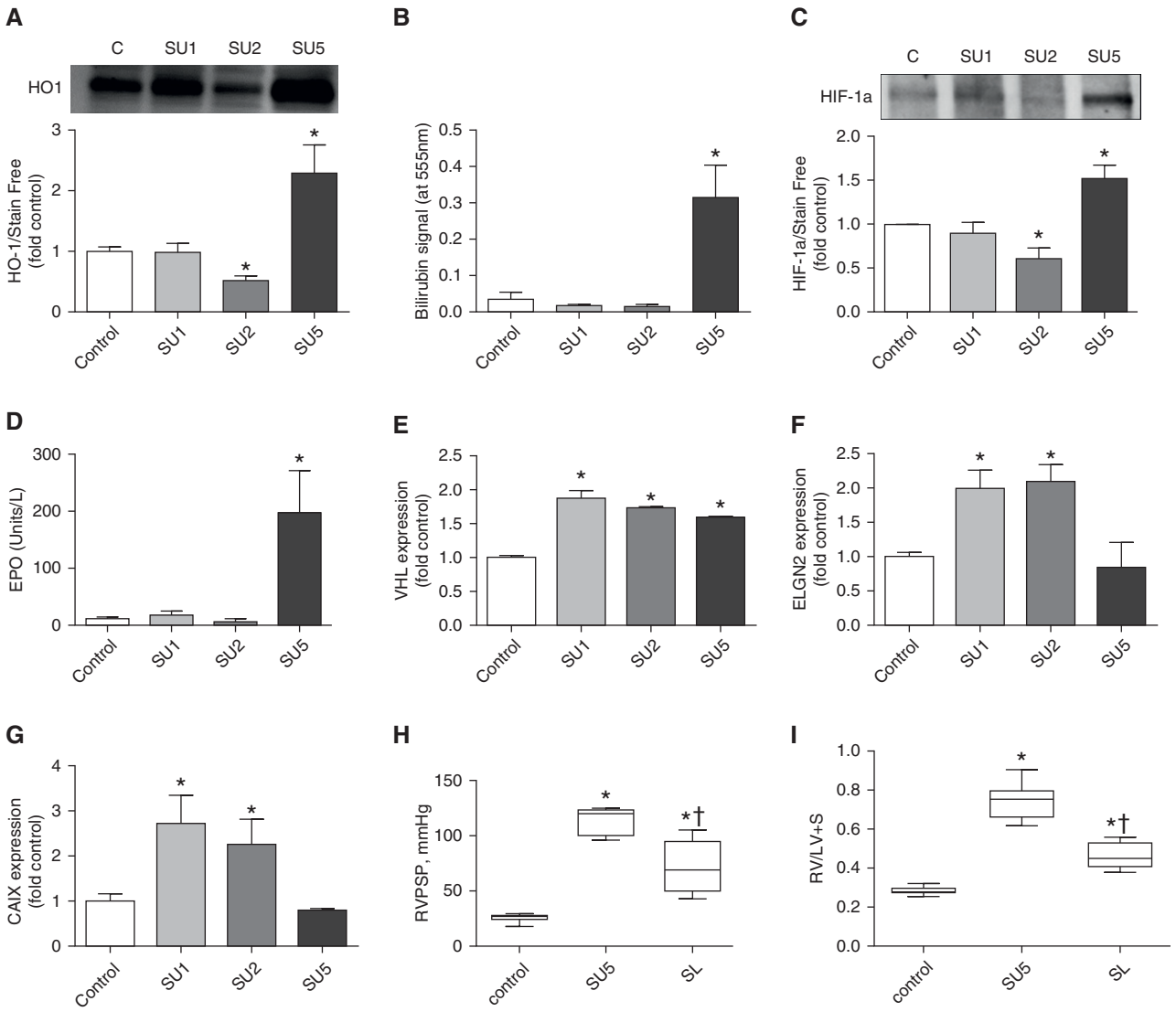


**Figure 7.** Heme oxygenase (HO) and HIF-1a pathways in the Su/hypoxia model. (*A*) We expected that heme-catabolizing HO would be induced at the early stage of the disease when heme-mediated pathways are fully active. In contrast, our data indicate no change in the SU1 group, and even decreased HO-1 expression in the SU2 group. Interestingly, HO-1 was highly expressed in the SU5 group. Gel loadings were normalized with the stain-free methods of total protein measurement; *see* Figure E2 (mean ± SEM, $^*P < 0.05$ versus control group, ANOVA, $n = 6$). (*B*) To ensure that HO activity was similar to the expression profile, we used bilirubin measurement in the lung tissue to assay HO-integral activity. Our data exhibited no increase in bilirubin level in the SU1 and SU2 groups and a highly elevated level in the SU5 group that correspond to our Western blot data (mean ± SEM, $^*P < 0.05$ versus control group, ANOVA, $n = 6$–8). (*C*) As HIF-1a regulates HO-1, we measured HIF-1a stability by Western blotting in the lung lysate. Surprisingly, the Western blot profile of HIF-1a was very similar to the HO-1 expression data. We found no activation of HIF-1a in the SU1 group and decreased stability in the SU2 group, despite the fact that rats were in the hypoxic condition for the first 3 weeks. Interestingly, HIF-1a was increased in the SU5 group that was in end-stage disease in normoxic settings. Loadings were normalized with the stain-free methods of total protein measurement; *see* Figure E1 (mean ± SEM, $^*P < 0.05$ versus control group, ANOVA, $n = 4$). (*D*) To exclude any possibility of artifactual results, we used erythropoietin (EPO) measurement as a reporter for HIF-1a activity. Again, we did not find an upregulation of EPO in the SU1 and SU2 groups, whereas SU5 had highly increased levels of EPO. This was very consistent with our Western blot data on the HIF-1a protein level in lungs (mean ± SEM, $^*P < 0.05$ versus control group, ANOVA, $n = 5$–8). Expression of (*E*) Von Hippel–Lindau (VHL) protein, which is responsible for degradation of HIF-1a, as well as (*F*) ELGN2, a protein that oxidizes proline residues in HIF-1a and targets it for degradation, were increased specifically in the first 2 weeks of the study (SU1 and SU2 groups; mean ± SEM, $^*P < 0.05$ versus control group, ANOVA, $n = 3$–4). (*G*) Importantly, expression of carbonic anhydrase IX (CAIX), which is an indicator of the hypoxic condition, independently exhibited hypoxic conditions in the first 2 weeks in the SU1 and SU2 groups (mean ± SEM, $^*P < 0.05$ versus control group, ANOVA, $n = 3$–4). (*H*) Treatment of rats with sulfasalazine (20 mg/kg) decreased RVPSP significantly and (*I*) heart hypertrophy (mean ± SEM, $^*P < 0.05$ versus control group, $^\dagger P < 0.05$ for SU5 versus SL, ANOVA, $n = 5$–8). RV / LV + S = right ventricle/left ventricle + septum.

### Inhibition of HCP-1–mediated Heme Entry in an SU/Hypoxia Model

To test whether intracellular heme signaling is directly involved in the development and progression of PAH in an animal model, we administer sulfasalazine (20 mg/kg intraperitoneally every 2 d) after 1 week from disease induction by Sugen injection and exposure to hypoxia (10% oxygen) and until Week 5. We found that inhibition of HCP-1 restored both RVPSP (Figure 7H) and the Fulton index (Figure 7I) if compared with the fully developed disease group (SU5).

## Discussion

Anemic conditions were previously shown to be associated with the severity of PAH (35). Free Hb released from RBCs can induce chronic vasoconstriction due to nitric oxide scavenging activity in the bloodstream (36). Elevated free Hb has also been described as an oxidant enzyme that induces oxidative stress, and this can damage the vasculature (37). Those pathways can certainly contribute to disease development via proliferative and fibrotic vascular remodeling. However, we observed that free heme released from free Hb could be a signaling molecule, which translates extracellular Hb effects into intracellular pathways.

In patients with PAH, we found strong correlations between extracellular Hb and main hemodynamic parameters, such as mPAP, PVR, and CI. Importantly, free Hb levels were elevated in PAH functional classes 3 and 4 that make it useful for prediction of disease progression. In the animal PAH model, we found that the early stage of disease development involves increased free Hb in plasma and decreased haptoglobin that indicates the enhanced rate of hemolysis. Free Hb releases heme, and lung microvascular endothelium is very sensitive to the rise of heme concentration, resulting in endothelial barrier dysfunction. Our animal data showed a significant increase in lung weight due to perivascular edema at the early stage of PAH. This is a very interesting observation, because perivascular fluid can decrease gas transport, leading to local hypoxia (38, 39), and induce vascular stiffness by mechanically restricting vasodilation. Thus, perivascular edema can explain why patients develop a local hypoxic microenvironment around the vessels and pulmonary artery stiffness, leading to RV dysfunction. Lung vasculature leakage increases immune cell infiltration, and this inflammatory component is also a well-established contributor to the progression of PAH (40). The previous study has shown that continuous intravenous administration of Hb in rats can mildly increase pulmonary pressure, leading to vascular remodeling and perivascular inflammation (21). Moreover, heme that crosses the endothelial barrier can directly affect proliferation of smooth muscle cells (41). Treatment with heme increased the smooth muscle cell proliferation via nitric oxide activation, with subsequent upregulation of reactive oxygen species–sensitive signaling pathways.

It was previously described that heme could affect NF-κB signaling through the activation of TLR4 (23). This typically leads to endothelial barrier disruption, as was very well documented for LPS-mediated action (24). However, LPS mediates a relatively slow endothelial barrier disruption, reaching its maximal effect roughly 3–4 hours after LPS exposure. In contrast, heme induces a very rapid effect, with maximum barrier break at 15 minutes after heme exposure. According to our data, heme can also induce a very acute signaling cascade through p38 MAPK and HSP27, leading to barrier dysfunction. We confirmed that this mechanism occurs in the animal model at early time points in the SU1 and SU2 groups, which correlated with increased leakage. Our work also sheds some light on the mechanism of heme uptake by the endothelial cell via HCP-1 (32). Our data indicate that, indeed, inhibition of HCP-1 dampens the heme-mediated intracellular activation of p38 MAPK. In fact, our animal data with sulfasalazine treatment indicate attenuation of PAH in the severe Su/hypoxia model. Thus, HCP-1 could be an important therapeutic target for heme-related complications.

HO is an inducible enzyme upon the increased concentration of heme. However, we did not find HO-1 induction at the early stage of disease in the SU1 and SU2 groups, but found a high level of HO-1 in the SU5 group. As HO is under HIF-1a control (42), it is expected to be activated during the hypoxic phase of our animal model. This activation of HO-1 has a very important physiological role, due to increased erythropoiesis in hypoxia, in overcoming reduced oxygen availability (43). Reticulocytes produced during hypoxia are more fragile than mature RBCs (44). Therefore, hypoxia can be associated with increased hemolysis. Interestingly, our data indicate decreased stability of HIF-1a during a hypoxic regimen for PAH induction in our animal model. In contrast, HIF-1a rose at Week 5 when rats returned to normoxia. Moreover, this was also confirmed by EPO measurements that rose at Week 5 as well. It is important to note that increased EPO levels were found in patients with PAH (26), and this correlates with our finding in the animal model. Interestingly, another marker of hypoxia, carbonic anhydrase IX, which is required for detoxification of $CO_2$, was increased at the exact time of hypoxic events, and decreased in normoxia. Destabilization of HIF-1a, at least in part, could be explained by upregulation of VHL and ENGL2 proteins, which are responsible for HIF-1a degradation. Moreover, another study linked free heme with destabilization of HIF-1a. It is also possible that free heme could destabilize HSP90/HIF-1a interaction and, therefore, reduce HIF-1a stability (45). Thus, the initial rise of heme at the early stage destabilizes HIF-1a, despite the hypoxic conditions, and this limits HO-1 induction. A possible role in HIF-1a stability was also shown for p38 MAPK. It was found that activity of p38 is opposed to HIF-1a stability, which resulted in HIF-1a activation by a p38 inhibitor (46). Indeed, HIF-1a in our study was inhibited when p38 was active at the first 2 weeks of the PAH animal model, with activation of HIF-1a at the late stage when p38 signaling was downregulated. HIF-1a activation without a hypoxia environment is well described for patients with PAH (47, 48), and results in increased erythropoiesis.

### Conclusions

This study found significant correlations between free Hb concentrations and PAH severity parameters, which can be a very useful tool in the clinic for predicting early onset of the disease. We discovered that heme-induced activation of the p38/HSP27 pathway results in increased lung vascular permeability, perivascular edema, and increased immune cell infiltration at the early stage of PH. These data pinpoint not only new biomarkers, but also new therapeutic targets for PAH. ■

**Author disclosures** are available with the text of this article at www.atsjournals.org.

## References


1. Gladwin MT, Machado RF. Pulmonary hypertension in sickle cell disease. *N Engl J Med* 2011;365:1646–1647. [Author reply, pp. 1648–1649.]
2. Kato GJ, Onyekwere OC, Gladwin MT. Pulmonary hypertension in sickle cell disease: relevance to children. *Pediatr Hematol Oncol* 2007;24: 159–170.
3. Rogers NM, Yao M, Sembrat J, George MP, Knupp H, Ross M, *et al*. Cellular, pharmacological, and biophysical evaluation of explanted lungs from a patient with sickle cell disease and severe pulmonary arterial hypertension. *Pulm Circ* 2013;3: 936–951.
4. Ussavarungsi K, Burger CD. Pulmonary arterial hypertension in a patient with β-thalassemia intermedia and reversal with infusion epoprostenol then transition to oral calcium channel blocker therapy: review of literature. *Pulm Circ* 2014;4:520–526.
5. Tofovic SP, Jackson EK, Rafikova O. Adenosine deaminase-adenosine pathway in hemolysis-associated pulmonary hypertension. *Med Hypotheses* 2009;72:713–719.
6. Belcher JD, Beckman JD, Balla G, Balla J, Vercellotti G. Heme degradation and vascular injury. *Antioxid Redox Signal* 2010;12: 233–248.
7. Lamb DC, Waterman MR, Kelly SL, Guengerich FP. Cytochromes P450 and drug discovery. *Curr Opin Biotechnol* 2007;18:504–512.
8. Jordan PM. Highlights in haem biosynthesis. *Curr Opin Struct Biol* 1994; 4:902–911.
9. Ferrer MD, Mestre-Alfaro A, Martínez-Tomé M, Carrera-Quintanar L, Capó X, Jiménez-Monreal AM, *et al*. Haem biosynthesis and antioxidant enzymes in circulating cells of acute intermittent porphyria patients. *PLoS One* 2016;11:e0164857.
10. Simoni J, Simoni G, Moeller JF. Intrinsic toxicity of hemoglobin: how to counteract it. *Artif Organs* 2009;33:100–109.
11. Rees DC, Williams TN, Gladwin MT. Sickle-cell disease. *Lancet* 2010; 376:2018–2031.
12. Machado RF, Gladwin MT. Pulmonary hypertension in hemolytic disorders: pulmonary vascular disease: the global perspective. *Chest* 2010;137(6 suppl):30S–38S.
13. Brauckmann S, Effenberger-Neidnicht K, de Groot H, Nagel M, Mayer C, Peters J, *et al*. Lipopolysaccharide-induced hemolysis: evidence for direct membrane interactions. *Sci Rep* 2016;6: 35508.
14. Irwin DC, Baek JH, Hassell K, Nuss R, Eigenberger P, Lisk C, *et al*. Hemoglobin-induced lung vascular oxidation, inflammation, and remodeling contribute to the progression of hypoxic pulmonary hypertension and is attenuated in rats with repeated-dose haptoglobin administration. *Free Radic Biol Med* 2015;82: 50–62.
15. Hooper WC, Mensah GA, Haworth SG, Black SM, Garcia JG, Langleben D. Vascular endothelium summary statement V: pulmonary hypertension and acute lung injury: public health implications. *Vascul Pharmacol* 2007;46:327–329.
16. Lin EE, Rodgers GP, Gladwin MT. Hemolytic anemia–associated pulmonary hypertension in sickle cell disease. *Curr Hematol Rep* 2005;4:117–125.
17. Mathew R, Huang J, Wu JM, Fallon JT, Gewitz MH. Hematological disorders and pulmonary hypertension. *World J Cardiol* 2016;8: 703–718.
18. Barnett CF, Hsue PY, Machado RF. Pulmonary hypertension: an increasingly recognized complication of hereditary hemolytic anemias and HIV infection. *JAMA* 2008;299: 324–331.
19. Wahl S, Vichinsky E. Pulmonary hypertension in hemolytic anemias. *F1000 Med Rep* 2010;2:pii:10.
20. Brittain EL, Janz DR, Austin ED, Bastarache JA, Wheeler LA, Ware LB, *et al*. Elevation of plasma cell–free hemoglobin in pulmonary arterial hypertension. *Chest* 2014;146:1478–1485.
21. Buehler PW, Baek JH, Lisk C, Connor I, Sullivan T, Kominsky D, *et al*. Free hemoglobin induction of pulmonary vascular disease: evidence for an inflammatory mechanism. *Am J Physiol Lung Cell Mol Physiol* 2012;303:L312–L326.
22. Belcher JD, Chen C, Nguyen J, Milbauer L, Abdulla F, Alayash AI, *et al*. Heme triggers TLR4 signaling leading to endothelial cell activation and vaso-occlusion in murine sickle cell disease. *Blood* 2014;123: 377–390.
23. Lin S, Yin Q, Zhong Q, Lv FL, Zhou Y, Li JQ, *et al*. Heme activates TLR4-mediated inflammatory injury via MyD88/TRIF signaling pathway in intracerebral hemorrhage. *J Neuroinflammation* 2012; 9:46.
24. Rafikov R, Dimitropoulou C, Aggarwal S, Kangath A, Gross C, Pardo D, *et al*. Lipopolysaccharide-induced lung injury involves the nitration-mediated activation of RhoA. *J Biol Chem* 2014;289:4710–4722.
25. Rafikova O, Rafikov R, Meadows ML, Kangath A, Jonigk D, Black SM. The sexual dimorphism associated with pulmonary hypertension corresponds to a fibrotic phenotype. *Pulm Circ* 2015; 5:184–197.
26. Karamanian VA, Harhay M, Grant GR, Palevsky HI, Grizzle WE, Zamanian RT, *et al*. Erythropoietin upregulation in pulmonary arterial hypertension. *Pulm Circ* 2014;4:269–279.
27. Plestina R, Stoner HB. Pulmonary oedema in rats given monocrotaline pyrrole. *J Pathol* 1972;106:235–249.
28. Molteni A, Ward WF, Ts'ao CH, Port CD, Solliday NH. Monocrotaline-induced pulmonary endothelial dysfunction in rats. *Proc Soc Exp Biol Med* 1984;176:88–94.
29. Ragab SM, Safan MA, Badr EA. Study of serum haptoglobin level and its relation to erythropoietic activity in beta thalassemia children. *Mediterr J Hematol Infect Dis* 2015;7: e2015019.
30. Garland P, Durnford AJ, Okemefuna AI, Dunbar J, Nicoll JA, Galea J, *et al*. Heme-hemopexin scavenging is active in the brain and associates with outcome after subarachnoid hemorrhage. *Stroke* 2016;47:872–876.
31. Alayash AI. Oxidative pathways in the sickle cell and beyond. *Blood Cells Mol Dis* 2018;70:78–86.
32. Latunde-Dada GO, Takeuchi K, Simpson RJ, McKie AT. Haem carrier protein 1 (HCP1): expression and functional studies in cultured cells. *FEBS Lett* 2006;580:6865–6870.
33. Ockaili R, Natarajan R, Salloum F, Fisher BJ, Jones D, Fowler AA III, *et al*. HIF-1 activation attenuates postischemic myocardial injury: role for heme oxygenase-1 in modulating microvascular chemokine generation. *Am J Physiol Heart Circ Physiol* 2005;289:H542–H548.
34. Haase VH. Regulation of erythropoiesis by hypoxia-inducible factors. *Blood Rev* 2013;27:41–53.
35. Machado RF, Farber HW. Pulmonary hypertension associated with chronic hemolytic anemia and other blood disorders. *Clin Chest Med* 2013;34:739–752.
36. Schaer CA, Deuel JW, Schildknecht D, Mahmoudi L, Garcia-Rubio I, Owczarek C, *et al*. Haptoglobin preserves vascular nitric oxide signaling during hemolysis. *Am J Respir Crit Care Med* 2016;193: 1111–1122.
37. Aphinives C, Kukongviriyapan U, Jetsrisuparb A, Kukongviriyapan V, Somparn N. Impaired endothelial function in pediatric hemoglobin e/β-thalassemia patients with iron overload. *Southeast Asian J Trop Med Public Health* 2014;45:1454–1463.
38. Zhou C, Townsley MI, Alexeyev M, Voelkel NF, Stevens T. Endothelial hyperpermeability in severe pulmonary arterial hypertension: role of store-operated calcium entry. *Am J Physiol Lung Cell Mol Physiol* 2016;311:L560–L569.
39. Tolstanova G, Deng X, French SW, Lungo W, Paunovic B, Khomenko T, *et al*. Early endothelial damage and increased colonic vascular permeability in the development of experimental ulcerative colitis in rats and mice. *Lab Invest* 2012;92:9–21.
40. Harbaum L, Baaske KM, Simon M, Oqueka T, Sinning C, Glatzel A, *et al*. Exploratory analysis of the neutrophil to lymphocyte ratio in patients with pulmonary arterial hypertension. *BMC Pulm Med* 2017; 17:72.
41. Moraes JA, Barcellos-de-Souza P, Rodrigues G, Nascimento-Silva V, Silva SV, Assreuy J, *et al*. Heme modulates smooth muscle cell proliferation and migration via NADPH oxidase: a counter-regulatory role for heme oxygenase system. *Atherosclerosis* 2012;224: 394–400.

42. Yang ZZ, Zou AP. Transcriptional regulation of heme oxygenases by HIF-1alpha in renal medullary interstitial cells. *Am J Physiol Renal Physiol* 2001;281:F900–F908.
43. Wheatley K, Creed M, Mellor A. Haematological changes at altitude. *J R Army Med Corps* 2011;157:38–42.
44. Liu J, Guo X, Mohandas N, Chasis JA, An X. Membrane remodeling during reticulocyte maturation. *Blood* 2010;115:2021–2027.
45. Lee JM, Lee WH, Kay HY, Kim ES, Moon A, Kim SG. Hemin, an iron-binding porphyrin, inhibits HIF-1$\alpha$ induction through its binding with heat shock protein 90. *Int J Cancer* 2012;130: 716–727.
46. Ryter SW, Xi S, Hartsfield CL, Choi AM. Mitogen activated protein kinase (MAPK) pathway regulates heme oxygenase-1 gene expression by hypoxia in vascular cells. *Antioxid Redox Signal* 2002;4:587–592.
47. Farha S, Asosingh K, Xu W, Sharp J, George D, Comhair S, *et al*. Hypoxia-inducible factors in human pulmonary arterial hypertension: a link to the intrinsic myeloid abnormalities. *Blood* 2011;117: 3485–3493.
48. Fijalkowska I, Xu W, Comhair SA, Janocha AJ, Mavrakis LA, Krishnamachary B, *et al*. Hypoxia inducible-factor1alpha regulates the metabolic shift of pulmonary hypertensive endothelial cells. *Am J Pathol* 2010;176:1130–1138.